www.czasopisma.pan.pl PAN POLSKA AKADEMIA NAUK www.journals.pan.pl

Arch. Metall. Mater., Vol. 61 (2016), No 2, p. 803–806

DOI: 10.1515/amm-2016-0135

A. DRYGAŁA*#, L.A. DOBRZAŃSKI*, M. SZINDLER*, M. PROKOPIUK VEL PROKOPOWICZ*, M. PAWLYTA*, K. LUKASZKOWICZ*

CARBON NANOTUBES COUNTER ELECTRODE FOR DYE-SENSITIZED SOLAR CELLS APPLICATION

The influence of the carbon nanotubes counter electrode deposited on the FTO glass substrates on the structure and optoelectrical properties of dye-sensitized solar cells counter electrode (CE) was analysed. Carbon materials have been applied in DSSCs in order to produce low-cost solar cells with reasonable efficiency. Platinum is a preferred material for the counter electrode because of its high conductivity and catalytic activity. However, the costs of manufacturing of the platinum counter electrode limit its use to large-scale applications in solar cells. This paper presents the results of examining the structure and properties of the studied layers, defining optical properties of conductive layers and electrical properties of dye-sensitized solar cells manufactured with the use of carbon nanotubes.

Such counter electrodes are promising for the future fabrication of stable, low-cost and effective dye-sensitized solar cells.

Keywords: dye-sensitized solar cells; counter electrode; carbon nanotubes; TEM.

1. Introduction

Solar energy is belong to a renewable source of energy that is sustainable, widely available and totally inexhaustible, unlike fossil fuels whose resources are being depleted. It is also a non-polluting source of energy and it does not emit any greenhouse gases during electricity producing [1-3]. The increasing demand for renewable energy due to recent issues like global warming, drastic climatic changes and the largely unexploited potential of the sun as an energy source made it as increasingly important, especially the solar energy conversion technology. Rapid progress in modern industries, including photovoltaics, depended mostly on the capabilities of materials forming and surface engineering [3-11].

A photovoltaic cell converts the energy from light directly into electricity by the photovoltaic effect. Solar cells are generally made from silicon or other semiconductors. When light quantum is absorbed, charge carriers may be generated by photons of energy greater then material band gap. Electrons struck by such photons break their covalent bonds in atoms, leave their positions and electron-hole pairs are generated. In the electric field of junction free electrons in the conduction band migrates toward the front surface and holes to the back surface. Electric current can flow through an external load when connected to cell's front and back contacts [1, 2, 4-7].

Dye-sensitized solar cells DSSC are an attractive alternative to conventional crystalline silicon solar cells because of its low-cost, relatively high photon-to-current conversion efficiency for low energy consumption and simple fabrication process [12]. The overall efficiency of ~12% [13] placed dye-sensitized solar cells as potential inexpensive alternatives to solid state devices. DSSCs are easy to manufacture using well known printing techniques. Moreover, dye-sensitized solar cells can be semi-transparent and semi-flexible, allowing a range of uses that are not applicable to the commonly known silicon-based photovoltaic wafer systems [2, 14].

The working principle of a DSSC (Fig. 1) substantially differs from that of a conventional solar cell based on silicon. Dye-sensitized solar cell are composed of: a nanostructured semiconductor (typically TiO_2), a dye to absorb visible light (mostly ruthenium complex), an electrolyte (e.g. containing I^-/I_3^- redox ions), which forms the interface with the semiconductor and a counter electrode leading an electrocatalyst, which helps the transfer of electrons to the liquid electrolyte [14-22].

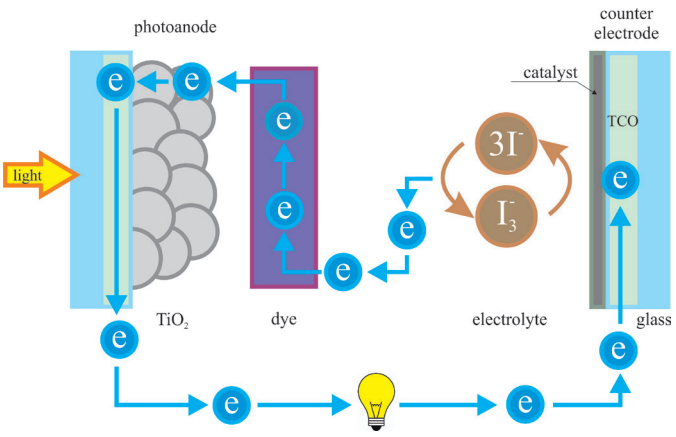

Fig. 1. Operating principle of dye-sensitized solar cell [2]

In DSSCs, the dye is a photoactive material which is excited by absorption of photons from light. The dyes inject this excited electron into the conductive band of titanium dioxide. The electrons flow through the outer electrical circuit to the counter electrode. The ionised dye molecules are then reduced by iodide ions in the electrolyte, which form triiodide ions. The counter electrode uses electrons that run from the

* SILESIAN UNIVERSITY OF TECHNOLOGY, INSTITUTE OF ENGINEERING MATERIALS AND BIOMATERIALS, 18A KONARSKIEGO STR., 44-100 GLIWICE, POLAND

Corresponding author: aleksandra.drygala@polsl.pl

working electrode to reduce triiodide ions back to iodide [24, 25]. Usually, platinum is used as the catalytic material and fluorine-doped thin oxide FTO glass as the substrate for counter electrode. Although Pt counter electrodes exhibit excellent catalytic and electric properties, they suffer from several limitations, e.g. high economic cost and difficulty in large-scale production [23-29].

In this paper multi-walled carbon nanotubes (MWCNTs) were used as alternative materials for platinum because of their special properties such as high corrosive resistance, high reactivity for triiodide reduction and low costs.

2. Materials and methodology

All reagents and solvents for synthesis were obtained from commercial sources and used without further purification. Multi-walled carbon nanotubes were purchased from CheapTubes.com. Polyvinylpyrrolidone PVP was obtained from Sigma- Aldrich.

Multi-walled carbon nanotubes (MWCNTs) were dispersed in anhydrous ethyl alcohol using a homogenizer. Carbon nanotubes are materials which strongly agglomerate. Therefore they were exposed to homogenization for 60 minutes. To prevent the aggregation of carbon nanotubes, the mixture of 95 wt.% of active material and 5wt.% of polyvinylpyrrolidone PVP was used. Then, using a droplet and spin coating methods, the mixture was deposited on conductive fluoride-doped tin oxide (FTO) coated glass substrates, having a sheet resistance of 7Ω/□. FTO glasses were cleaned with distilled-water, acetone, isopropyl alcohol and ethanol alcohol by ultrasonication. For fabricating photoanodes, highly dispersed titania nano-particle paste (Ti-Nano oxide T/SP, Solaronix) was used to form the transparent active layer. The TiO_2 layer was screen-printed onto FTO glass. Next The TiO_2 coated FTO glass was dried at 120°C for 5 min and then another layer was printed until three layers were obtained. To remove the organic screen printing vehicle and to enhance electron transport three layers of titania coated FTO glass was fired at 500°C (with a slow temperature ramp - 30°C per minute) under an inert atmosphere and maintain for 30 minutes. Photoanode was preheated at 80°C for 30 min before it was immersed in 0.5 mM ethanol solution of cis-diisothiocyanato-bis (2.2'-bipyridyl-4.4'-dicarboxylic acid) ruthenium (II) known as N3 at room temperature for 24h. General platinum-based counter electrodes were also prepared by screen printing method following by thermal treatment at 500°C for 30 min as references. The internal space between the TiO_2 photoanode and counter electrode was controlled to be 25 µm by thick hot melt sealing foil. The electrolyte used in this study was iodide/tri-iodide redox couple with redox concentration of 150 mM consisted of an ionic liquid, alkyl benzimidazole, thiocyanate in 3-methoxy propionitrile (Iodolyte Z-150, Solaronix). The sandwich-type dye-sensitized solar cells with an active area of 0.54 cm^2 defined by screen mesh during screen printing method were used to compare cell performance.

The morphology of the carbon nanotubes surface was performed using a scanning electron microscope Zeiss Supra 35. The accelerating voltage was 5 kV. In order to obtain images of the surface topography the detection of secondary electrons by the detector In Lens was used. The detailed structural studies were made using a scanning-transmission electron microscope S/TEM Titan 80-300 of FEI Company. For this purpose, prepared carbon nanotubes were deposited on the special copper mesh used in electron microscopy. The whole study was complemented by a Raman spectroscopy. The device provides information about the structure of the molecule, that is, the mutual connection atoms in the molecule. Its great advantage is the non-destructive nature of the analysis of the sample.

The transmittance of carbon nanotubes layer deposited by droplet and spin coating method was measured by Thermo Scientific Evolution 220 spectrophotometer. Electrical parameters of manufactured dye-sensitized solar cells with platinum and carbon nanotubes counter electrode were characterised by measurements of I-V illuminated characteristics on PV Test Solutions Tadeusz Żdanowicz Solar Cell I-V Tracer System under standard AM 1.5 radiation.

3. Results and discussion

The Figures 2a and 2b shows the topography of the carbon nanotubes surface deposited on FTO glass. The deposited carbon nanomaterials are characterised by a fibrous structure without any damage and contamination. Produced surface layers are composed of carbon nanotube, whose diameters do not exceed 20 nm. Estimating the diameter of the nanotubes was only possible at high magnification. For this purpose ImageJ software was used.

a) b)

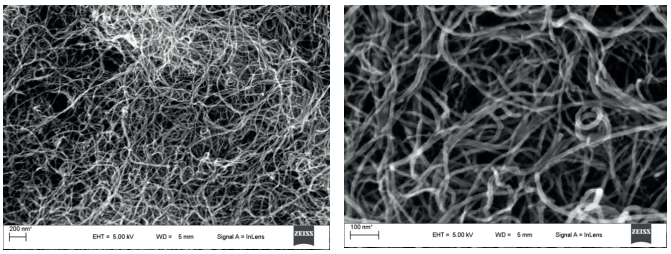

Fig. 2. SEM images of carbon nanotubes surface topography

Investigations of the transmission electron microscope were done to confirm that the produced surface layers are made from multi-walled carbon nanotubes. The investigated nanotubes are homogenous, and their diameter is about 10-14 nm, which is well visible in a TEM image (Fig. 3a). The results also confirm that the analysed material is pure, i.e. deprived of metallic impurities and amorphous carbon deposits. It can be seen based on the image made with the HAADF detector in the STEM mode that there are some impurities arranged on the surface of carbon nanotubes. Visible on the left corner nanoparticle (Fig. 3b) is discernible on the images as a clearly dark precipitate.

The Raman spectrum of carbon nanotubes sample was recorded (Fig. 4). The results were processed using the programme WiRETM 3.1. The G peak is a peak ranging from planes of graphite (sp^2 structure), and D is the diamond peak (sp^3). The ratio of the area under the D peak to the field contained in a G peak determines the degree of crystallisation

(I_D/I_G), and after that the structural construction of nanotube (Table 1). For the observed sample have not been registered a Radial Breathing Mode peak (RBM) - characteristic for single-wall nanotubes. The observed sample represents a multi-walled carbon nanotubes.

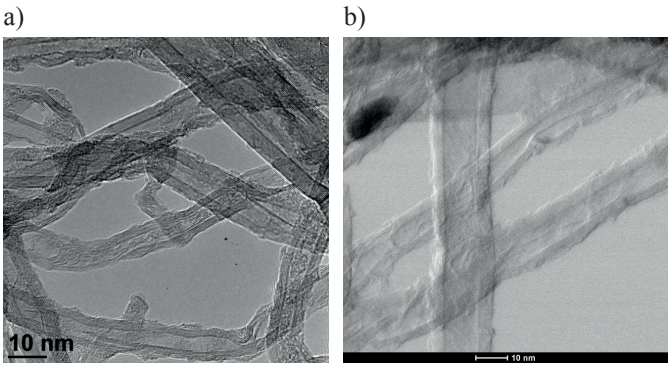

Fig. 3. TEM (a) and HAADF-STEM (b) carbon nanotubes images

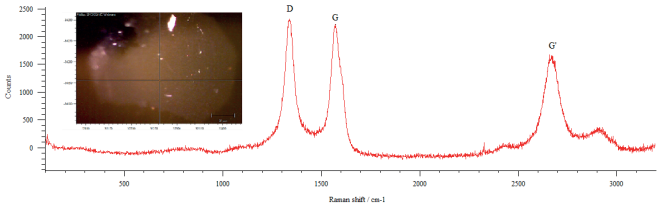

Fig. 4. Raman spectra of multi-walled carbon nanotubes

Optical properties of carbon nanotubes layer deposited by droplet and spin coating were characterised by transmittance over the wavelength range from 200 nm to 1100 nm. In Fig. 5 transmittance of particular layer method is shown. At a range of 300 nm – 400 nm all substrates presented a low value of transmittance but rised gradually through the visible region. The largest transmittance has FTO glass substrate without nanotubes layer. It has been found that counter electrode prepared from carbon nanotubes layer deposited by spin coating method exhibits a higher transmission of the light compared to droplet method. Because of that dye-sensitized solar cell was prepared only with carbon nanotubes counter electrode deposited on FTO glass by spin coating method.

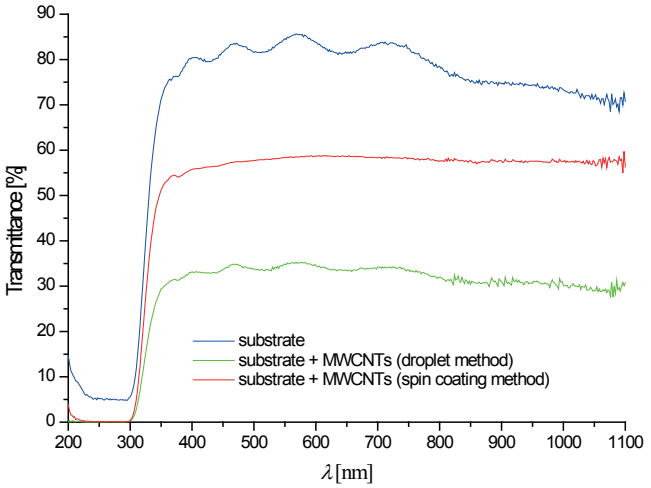

Fig. 5. Transmittance of carbon nanotubes layer

Fig. 6. depicts the current-voltage characteristics at AM 1.5 illumination for dye-sensitized solar cells with platinum and carbon nanotubes counter electrode. Electrical properties of manufactured dye-sensitized solar cells determined from I-V characteristics are given in the Table 2. Dye-sensitized solar cell with carbon nanotubes counter electrode demonstrates slightly worse electrical performance than cells with platinum. DSSCs manufactured with MWCNT counter electrodes obtained an efficiency of 1.97%. This efficiency was comparable to that of the conventional Pt-based dye-sensitized solar cell (2.53%).

TABLE 1

Results of Raman spectroscope research for pristine MWCNTs

*	Raman shift [cm^{-1}]	Intensity	Area
G	1572,84	2182,68	167905
D	1338,19	2149,86	224268
G'	2672,04	1658,44	205856
ID/IG ratio	1,34		

TABLE 2

The electrical properties of dye-sensitized solar cells with platinum and carbon nanotubes counter electrode

Counter electrode	Electrical properties						
	U_{OC} [mV]	I_{SC} [mA]	I_m [mA]	V_m [mV]	P_m [mW]	FF	E_{ff} [%]
Platinum	629.99	3.81	3.13	433.12	1.36	0.53	2.53
Carbon nanotubes deposited by spin coating method	626.23	3.14	2.332	381.95	0.89	0.49	1.97

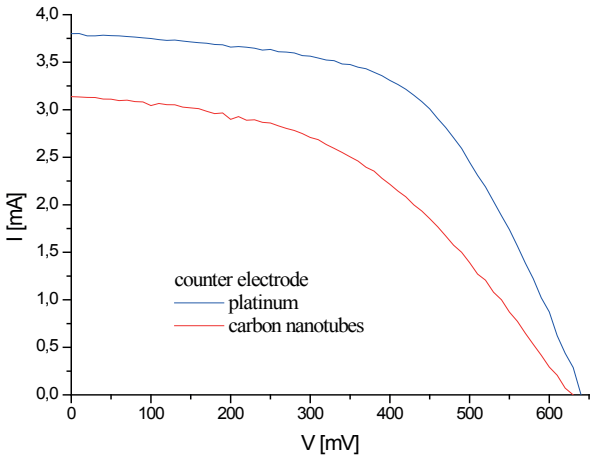

Fig. 6. Current-voltage characteristics of dye-sensitized solar cells manufactured with platinum and carbon nanotubes counter electrode

4. Conclusions

TEM and SEM studies have confirmed that a layer of carbon nanotubes was produced without major contamination and damage. The deposited carbon nanomaterials are characterised by a fibrous structure, whose diameters do not exceed 20 nm. The Raman spectrum has confirmed that the observed sample represents a multi-walled carbon nanotubes with good quality. It has been found that counter electrode prepared from carbon nanotubes layer deposited by spin coating method demonstrates higher transmission of the light compared to droplet method. The electrical properties of dye-sensitized solar cells with carbon nanotubes layer (deposited by spin coating method) as the counter electrode are lower but close to the performance of cell using conventional platinum as the counter electrode. Such electrodes give a possibility of the future fabrication of stable, low-cost and effective dye-sensitized solar cells.

Acknowledgment

The project was funded by the National Science Centre on the basis of the contract No. DEC-2013/09/B/ST8/02943. This publication was co-financed by the Ministry of Science and Higher Education of Poland as the statutory financial grant of the Faculty of Mechanical Engineering SUT.

REFERENCES

[1] S. Al-Hallaj, K. Kiszynski, Renewable Energy Sources and Energy Conversion Devices, Green Energy and Technology, Springer-Verlag, London (2011).

[2] J. Bisquert, D. Cahen, G. Hodes, S. Rühle, A. Zaban, J. Phys. Chem. B **108**, 8106-8118 (2004).

[3] V.V. Tyagi, N.A.A. Rahim, N.A. Rahim, J.A.L. Selvaraj, Renew. Sust. Energ. Rev. **20**, 443-461 (2013).

[4] G. Kulesza, P. Panek, P. Zieba, Arch. Civ. Mech. Eng. **14**, (4), 595-601 (2014).

[5] L.A. Dobrzański, A. Drygała, Mater. Sci. Forum **706-709**, 829-834 (2012).

[6] B. Swatowska, T. Stapinski, K. Drabczyk, P. Panek, Opt. Appl. **41**, (2), 487-492 (2011).

[7] L.A. Dobrzański, T. Tański, A. Dobrzańska-Danikiewicz, E. Jonda, M. Bonek, A. Drygała, Structures, properties and development trends of laser-surface-treated hot-work steels, light metal alloys and polycrystalline silicon, in: J. Lawrence, D. G. Waugh (Ed.), Laser surface engineering: Processes and applications, Elsevier, Amsterdam (2015).

[8] S. Lesz, R. Babilas, R. Nowosielski, Solid State Phenom. **203-204**, 296-301 (2013).

[9] L.A. Dobrzański, K. Lukaszkowicz, A. Kriz, J. Mater. Process. Tech. **143**, 832-837 (2003).

[10] M.U. Uysal, M. Kremzer, Acta Phys. Pol. A **127**, (4), 1355-1357 (2015).

[11] L.A. Dobrzański, M. Szindler, A. Drygała, M.M. Szindler, Cent. Eur. J. Phys. **12**, (9), 666-670 (2014).

[12] A. Sedghi, H.N. Miankushki, Int. J. Electrochem. Sc. **9**, 2029-2037 (2014).

[13] M.A. Green, K. Emery, Y. Hishikawa, W. Warta, E.D. Dunlop, Prog. Photovoltaics **23**, (7), 805-812 (2015).

[14] E. Stathatos, J. Eng. Sci. Technol. Rev. **5**, (4), 9-13 (2012).

[15] K.S. Lee, W.J. Lee, N.G. Park, S.O. Kim, J.H. Park, Chem. Commun. **47**, 4264-4266 (2011).

[16] H.C. Weerasinghe, F. Huang, Y. Cheng, Nano Energy **2**, (2), 174-189 (2013).

[17] M. Grätzel, J. Photoch. Photobio. C **4**, 145-153 (2003).

[18] S.A. Song, M.J. Lim, K.Y. Jung, W.-W. So, S.-J. Moon, Arch. Metall. Mater. **60**, (2), 1467–1471 (2015).

[19] M. Wu, T. Ma, J. Phys. Chem. C **118**, (30), 16727-16742 (2014).

[20] Z. Tang, J. Wu, M. Zheng, J. Huo, Z. Lan, Nano Energy **2**, (5), 622-627 (2013).

[21] X. Ma, G. Yue, J. Wu, Z. Lan, Nanoscale Res. Lett. **10**, 327 (2015).

[22] S. Thomas, T.G. Deepak, G.S. Anjusree, T.A. Arun, S.V. Nair, A.S. Nair, J. Mater. Chem. A **2**, 4474-4490 (2014).

[23] H. Anwar, A.E. George, I.G. Hill, Sol. Energy **88**, 129-136 (2013).

[24] J. Chen, B. Li, J. Zheng, J. Zhao, Z. Zhu, J. Phys. Chem. C **116**, (28), 14848-14856 (2012).

[25] T. Sawatsuk, A. Chindaduang, C. Sae-Kung, S. Pratontep, G. Tumcharern, Diam. Relat. Mater. **18**, 524-527 (2009).

[26] C.-T. Hsieh, B.-H. Yang, Y.-F. Chen, Diam. Relat. Mater. **27-28**, 68-75 (2012).

[27] H. Desilvestro, Y. Hebting, M. Khan, D. Milliken, Mater. Matt. **9**, (1), 14-18 (2014).

[28] L.A. Dobrzański, M. Bonek, M. Piec, E. Jonda, Mater Sci Forum. 532-533, 657-660 (2006).

[29] M. Bonek, L.A. Dobrzański, Mater Sci Forum. 654-656, 1848-1851 (2010).